ORIGINAL RESEARCH PAPER

Investigation on the photocatalytic activity of chemically synthesized zirconium doped cadmium selenide nanoparticles for indigo carmine dye degradation under solar light irradiation

Emelda Rayappan[1], Jayarajan Muthaian[2], Muthirulan Pandi[3]*

[1,2]Department of Chemistry, Annai Velankanni College (Affiliated to Manonmaniam Sundaranar University, Tirunelveli – 627012), Tholayavattam-629157, TN, India
[3]Department of Chemistry, Lekshmipuram College of Arts and Science (Affiliated to Manonmaniam Sundaranar University, Tirunelveli – 627012), Neyyoor-629802, TN, India

ABSTRACT

A simple chemical methodology has been adopted for the synthesis of zirconium (Zr) doped and un-doped cadmium selenide (CdSe) nanoparticles for the application towards photocatalytic degradation of indigo carmine (IC) dye under solar light irradiation. The Zr-CdSe (doped) and CdSe (un-doped) nanoparticles were characterized by ultraviolet-visible spectroscopy (UV-vis), X-ray diffraction (XRD), Scanning electron microscopy (SEM) coupled with energy dispersive X-ray analysis (EDAX), and Transmission electron microscopy (TEM) studies. The inclusion of Zr ion into the CdSe nanoparticles matrix was confirmed by SEM-EDAX and XRD studies. TEM studies confirm the zirconium ions are uniformly doped over the CdSe surface. The photocatalytic degradation performance of Zr doped and un-doped CdSe nanoparticles was examined for the degradation of IC dye under solar light irradiation. The experimental results indicated that the Zr-doped CdSe possessed greater photocatalytic activity in comparison to un-doped CdSe. Photodegradation process parameters such as the initial concentration of the dye, as well as the amount of catalyst and time were investigated. The photocatalytic degradation rate was favored by a high concentration of the solution in respect to Langmuir–Hinshelwood model.

Keywords: *Zr doped CdSe nanoparticles, indigo carmine dye, solar irradiation, photodegradation*

INTRODUCTION

Today, in the 21st century, there is still a lack of global concern about the sustainable source of energy and its ever-growing demand. Organic dyes, which are employed in industries such as paints, textiles, plastics, tannery, and printing industries are complex molecules. Currently, more than 10 million different dyes amounting to 7×10^5 tones are produced globally every year. Approximately 12-15% of the dyes applied in the manufacturing activities are discharged through the effluent as they are not entirely fixed. In recent years, there is a growing concern about the environmental pollution caused by inadequately treated dye-bearing industrial effluents. Most of these dyes are resistant to biodegradation and endanger living organisms, particularly when released in water bodies. Accumulation of intensely colored dyes in water bodies restricts the penetration of sunlight, hinders the circulation of oxygen, promotes eutrophication, and eventually compromises the
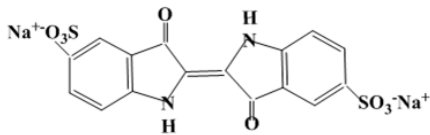
* Corresponding Author Email: *pmuthirulan@gamil.com*

Table 1. Molecular Structure and Chemical properties of Indigo Carmine dye

Dye	Indigo Carmine
Formula	$C_{16}H_8N_2Na_2O_8S_2$
Characteristics	Water soluble
Structure	
Molecular weight	466.36g/mol
λ_{max}	610nm
Application	Nylon, Wool, Polyester

natural trend of aquatic life. Hence, there is an immense need for the complete removal of these dyes from the contaminated water bodies using some effective techniques. The photocatalysis augmented by nanoparticle catalysts could be considered as a suitable method to meet such a need [1-4].

Extensive research activity in the field of photocatalysis involving semiconductor nanoparticles under visible light is seen. The major benefit of preferring this technique of photocatalytic degradation is its ability to employ the energy from solar radiation to produce hydroxyl radical (OH·) for dye degradation [5-7]. Earlier, different tactics were put into use for enhancing their photocatalytic activity that includes the surface modification, doping of transition or non-transition metallic ions, and the immobilization of nanoparticles into solid support [8-10]. The Indigo Carmine (IC) dye is regarded as one of the exceptionally virulent indigoid classes of the dye which marks one of the largest collections of toxic pollutants present in wastewater from textile and other industries. These compounds are classified as environmental toxicants as disposal of this colored polluted water into the life-supporting bodies causes problems such as esthetic pollution and the disorder of aquatic life form [11, 12]. IC is released into the water after its processing as it is among the most widely used textile dyeing agents. Its usage could be found in many areas such as an additive in tablets and capsules in pharmaceutical industries, in analytical chemistry, it is used as a redox indicator, as a microscopic stain in biology, and in various other applications [13].

Most of the earlier studies in the research area of organic dye pollution remediation have explored the catalytic ability of nanocomposites or metal oxide nanoparticles on the degradation of selected dyes. Studies comparing the augmenting potentials of transition metal nanoparticles in the photocatalysis of organic dyes are scanty. CdSe, an n-type semiconductor finds a wide range of applications in catalysis as it is having a band-gap in visible light (1.6eV-1.8eV) [14, 15], biological labeling [16], and solar cells [17]. CdSe has been regarded as an efficient semiconductor under visible light irradiation [18]. However, the fast recombination of photo-generated electron-holes restricted its practical application because the photo-induced electrons and holes are neutralized before they could initiate the photocatalytic process [19]. Recently, doping non-metals as a replacement to improvise the visible light response to metal oxide semiconductors has been employed [20-22]. By modifying the electronic structure of semiconductor and doping the non-metals, the bandgap could be narrowed [21, 23, 24]. Therefore, this study was carried out to explore the synthesis of CdSe and Zr doped CdSe for the application towards the degradation of acidic dye namely indigo carmine dye under solar light irradiation in an aqueous medium.

MATERIALS AND METHODS
Chemicals and Reagents
All the chemicals are purchased from LOBA Chemie, India, and used as received. The molecular structure and chemical properties of IC dye are given in Table 1.
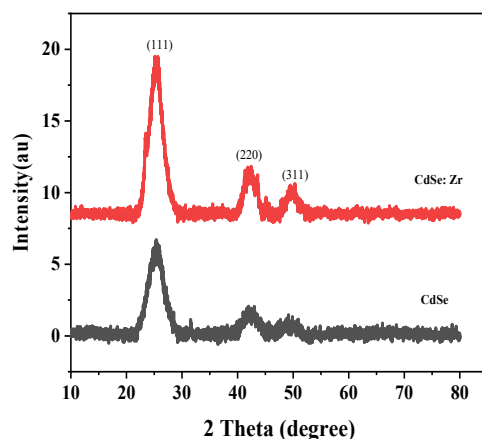
178

J. Water Environ. Nanotechnol., 6(2): 177-187 Spring 2021

Fig. 1. XRD pattern of CdSe and Zr-CdSe nanoparticles

Preparation of Zr doped CdSe nanoparticles

0.1M cadmium chloride and 0.1M sodium selenite solutions were prepared using deionized water in the presence of 0.3M mercaptoacetic acid and mixed in a beaker. The pH of the solution was adjusted in the range 7 to 8 and 0.04M zirconium oxychloride solution was added into the above mixture by dropwise addition. later on, the mixed solution was allowed to be stirred for 2 hours at room temperature. The appearance of the red color solution is the indication for the formation of Zr doped CdSe nanoparticles and precipitated out by the dropwise addition of propanal and the resulting red precipitate obtained was filtered [24].

Characterization techniques

The phase identification of the CdSe and Zr-CdSe nanoparticles was characterized using **BRUKER D8 ADVANCE** powder XRD with Cu =Kα (λ=1.5418Å) radiation. UV-Vis was analyzed with the help of **AGILENT 5000** UV -Vis spectrophotometer in the spectral range between 200nm to 800nm. Surface Morphology and Elemental analysis were scanned by **Jeol 6390LA/ OXFORD XMX N** instrument.

Photodegradation analysis

Photocatalytic activity of the Zr doped and un-doped CdSe nanoparticles was investigated by the degradation of indigo carmine dye in an aqueous solution under solar light irradiation and the experiment was carried out between 11.30 am and 12.00 pm in the summer season at Annai Velankanni College, Tholayavattam, Kanniyakumari, India. During this period, solar intensity fluctuation was reduced.

2000 (ppm) stock solution of IC dye was prepared [25]. The desired concentration (5-50ppm) was diluted using the stock solution. 20ml of the dye solution of required concentration along with 20mg of catalyst was added and subjected to irradiation under solar light. To ensure proper and complete mixing of catalysts, the beakers were stirred continuously using a magnetic stirrer. At the pre-determined time intervals, measured portions of the sample were taken and analyzed after centrifugation. The concentration of the dye was found, using a photo calorimeter at λ_{max}- 610nm.

Percentage removal (%R) =100*C_i-C_f/C_i

Where C_i is the initial concentration of dye (ppm), C_f is the final concentration of dye (ppm) at a given time.

RESULTS AND DISCUSSION

XRD analysis

XRD spectra of the zirconium doped and un-doped CdSe nanoparticles are shown in Fig. 1. The broad diffraction peaks in the XRD pattern of the productive sample could be well indexed by (111), (220), and (311) plane reflection [JCPDS No.09-0191]. This indicates that both the NPs are cubic phase crystalline structures with a preferred direction of the (111) plane [26-28]. Moreover, the intensity of Zr doped CdSe NPs is slightly greater than that of undoped CdSe NPs which confirms the doped NPs having a highly crystalline nature.

The average crystallite size of the NPs was assessed by the Debye Scherer formula [29]

$D=K\lambda/\beta Cos\theta$

Where D is the average crystallite size, β is the full width at half maximum (FWHM) of the

J. Water Environ. Nanotechnol., 6(2): 177-187 Spring 2021

179

Table 2. Different parameters of CdSe and CdSe: Zr Nanoparticles calculated from XRD spectrum

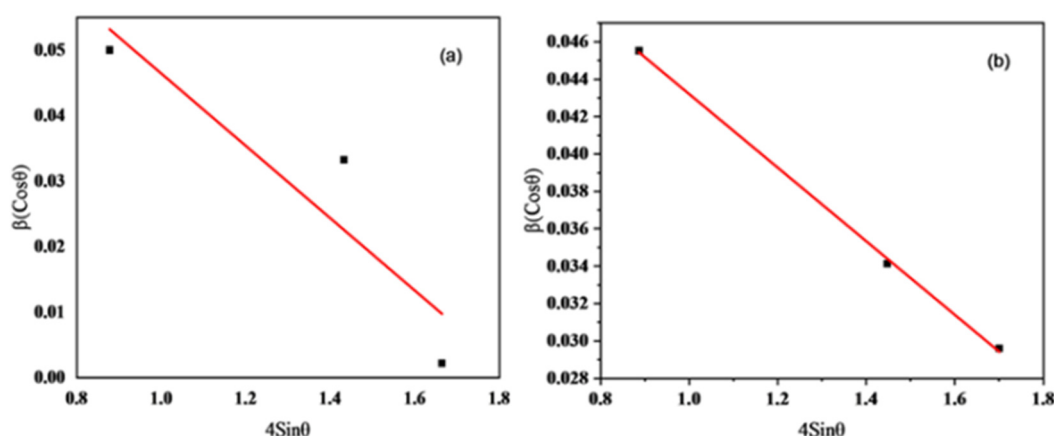| Sample	2θ (degree)	FWHM (degree)	Matching Peaks	d(Å)	Lattice Constant (a)	Crystallite Size(nm)	Average Crystallite (nm)	Density Dislocation δ (Å)
CdSe	25.3630	2.9380	(111)	3.5088	5.26326	2.7	23	0.189
	41.9739	2.0429	(220)	2.1507	6.08309	4.1		
	49.1746	0.1367	(311)	1.8513	6.14006	63.9		
CdSe: Zr	25.6289	2.6760	(111)	3.4730	6.01541	3.0	3.8	6.925
	42.4440	2.0993	(220)	2.1280	6.01889	4.0		
	50.3406	1.8755	(311)	1.8111	6.00673	4.6		

Fig. 2. Williamson-Halls plot of CdSe (a) and Zr-CdSe (b) nanoparticles

diffraction peak, λ (0.1541nm) is the wavelength of X-ray radiation and θ is the angle of diffraction [30]. The average particle size was found to be 23nm and 3.8nm for CdSe and Zr doped CdSe NPs respectively. In addition, the size of Zr doped CdSe NPs have decreased with the concentration increase and their crystalline size was less than that of the pure CdSe NPs. Besides, the doping size was decreased due to the inclusion of Zr ion into CdSe lattice, which decreases the grain's growth [31].

The inter planar distance spacing (d) of lattice plane is determined from Bragg's relation

$n\lambda = 2dSin\theta$

Where λ=1.5406Å and θ is Bragg diffraction angle. The structural parameters of CdSe and Zr-CdSe NPs are evaluated from the XRD data given in Table 2.

The lattice parameter (a) of cubic crystallite structure is determined by using the following relation,

$a = d (h^2+k^2+l^2)^{1/2}$

Where d is the interplanar distance (Å) and (hkl) are the miller indices of the planes.

The dislocation density is the length of dislocation lines per unit volume of the crystal [32]. Dislocation is a crystallographic irregularity or ugliness within a crystal structure and it could change the characteristics of materials. The dislocation density (δ) is determined from Williamson- Smallman relation, using the expressions:

$\delta = 1/D^2$

Where D is the average particle size. The dislocation density value obtained from the Scherer method is 0.189Å and 6.925Å for pure and CdSe: Zr NPs.

Crystallite Size and Strain are calculated from the Williamson Hall plot as shown (Fig. 2(a) and (b). It is plotted against the βCosθ versus Sinθ gives a straight line, the slope value indicates the amounts of residual strain (ε) and the reciprocal of intercept gives the average particle size [33, 34]. W-H plot gives a negative slope value due to the presence of compressive strain [35]. It could be noted from the W-H plot that the strain increases from -0.0553 to -0.0197 as the grain size decreases from 19.7nm to 3.9nm for pure and CdSe: Zr NPs. When Compared to the Scherer method and
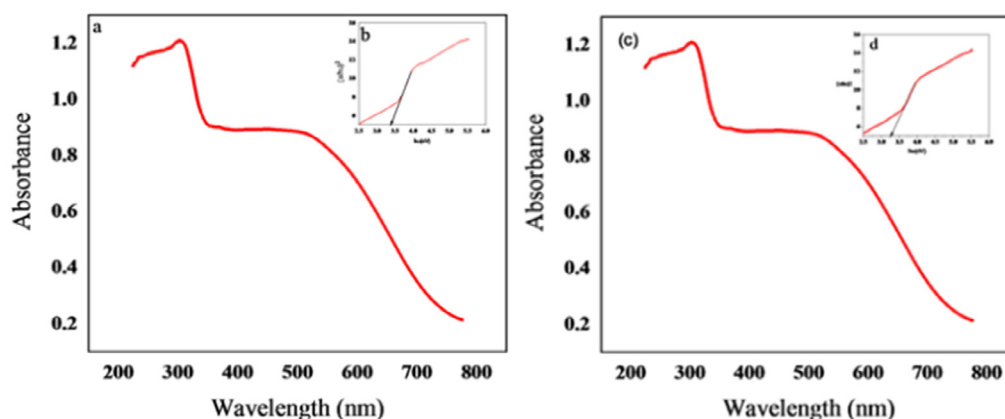
Fig. 3. UV spectrum CdSe (a) and Zr-CdSe (c) nanoparticles: Inset Tauc plot (b, c)

Williamson Hall method, the grain size was almost close to each other.

Optical studies

UV-Visible absorption spectra of the CdSe and Zr-CdSe nanoparticles were shown in Fig. 3 (a) and (b): inset is Tauc plot. The absorption peak at 300nm was observed for CdSe and Zr-CdSe nanoparticles and Zr doped CdSe nanoparticles showed a slight blue shift [36].

The optical transition energy was calculated from the absorption spectra using the Tauc relation [37, 38] which is expressed as

$$(\alpha h v) = A (h v - E_g)^r$$

Where A is the constant, α is the absorption coefficient, h*v* is the photon energy, E_g is the optical band gap, r is an index that relies on the nature of electronic transition responsible for optical absorption. The value of r is ½ for direct transition and 2 for indirect transition. Hence for direct transition becomes:

$$(\alpha h v) = A (h v - E_g)^{1/2}$$

By extrapolating the linear region of the plot of h*v* vs. (αh*v*), the value of the optical band gap could be found in Fig. 3 (Inset). The bandgap energy (E_g) of Zr doped and un-doped CdSe NPs was found to be 3.37eV, 3.24eV, which exceeds the value of the bulk CdSe bandgap (E_g=1.74eV).

SEM -EDAX and TEM analysis

SEM-EDAX studies provided information about surface morphology and the elemental of the CdSe and zirconium doped CdSe nanoparticles. The SEM-EDAX spectra of the CdSe and Zr-CdSe are shown in Fig. 4. The surface morphology of the CdSe nanoparticles was observed highly agglomerated bigger in size particles. In contrast, the surface morphology of the Zr-doped CdSe nanoparticles indicated smaller in size with reduced agglomeration (Fig. 4(a) and (c). The inclusion of the Zr onto the CdSe matrix was confirmed by the EDAX image (Fig. 4(b) and (d). The percentage composition of the elements for Zr doped and undoped nanoparticles is given in Table 3.

TEM images of the CdSe and zirconium doped CdSe nanoparticles are shown in Figs. 5(a) and (b). It was observed from the figure that the synthesized doped and un-doped CdSe nanoparticles are in nanometer size as well as the zirconium ions are well doped/included or dispersed into the CdSe matrix, besides some of the particles are agglomerated. Fig. 5(c) shows the selected area of electron diffraction (SAED) of Zr-CdSe nanoparticles. SAED patterns consist of three diffraction ring were indexed with (111), (220) and (311) plane of crystalline structure [39, 40]. The diffraction ring was consonant with the powder XRD spectrum of the diffraction peak.

INVESTIGATION ON THE PHOTOCATA-LYTIC ACTIVITY OF CdSe AND Zr-CdSe NANOPARTICLES

Effect of initial dye concentration IC dye

The photocatalytic degradation of IC dye was carried out under solar light illumination at different initial concentrations of the dye from 5ppm to 50ppm and a fixed dosage of catalyst (20mg of CdSe and Zr-CdSe NPs) and time (45min). Fig. 6 shows the percentage of degradation decrease with an increase in the initial concentration of IC dye from 40% to 16% for CdSe and 60% to 31% for Zr-CdSe NPs. This is maybe due to:

1. A large number of dye molecules adsorbed on

Element	Line Type	Wt%	Atomic %
Se	L series	37.58	46.15
Cd	L series	62.42	53.85
Total:		100	100

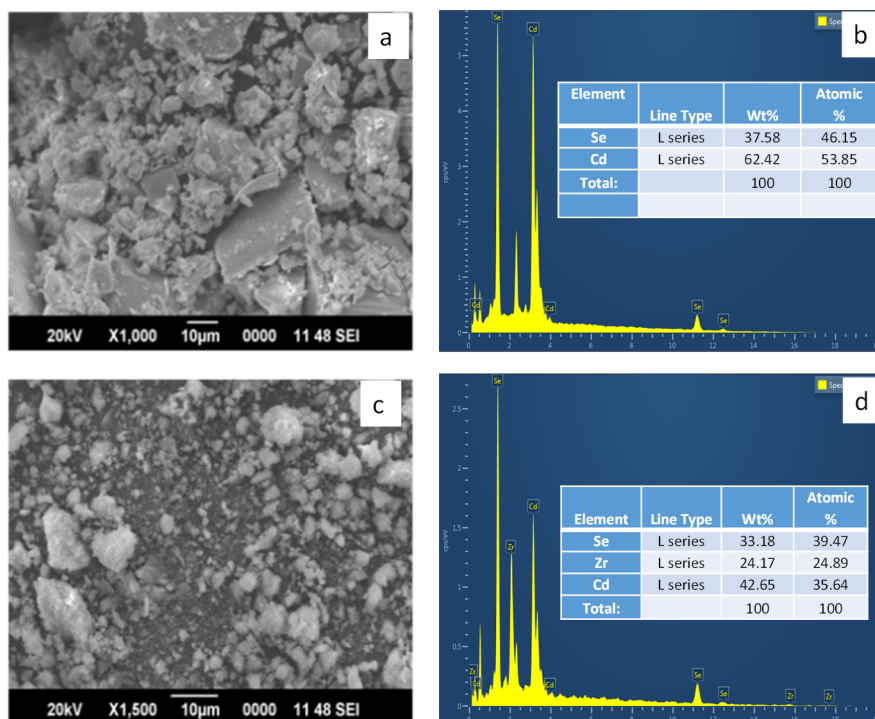| Element	Line Type	Wt%	Atomic %
Se	L series	33.18	39.47
Zr	L series	24.17	24.89
Cd	L series	42.65	35.64
Total:		100	100

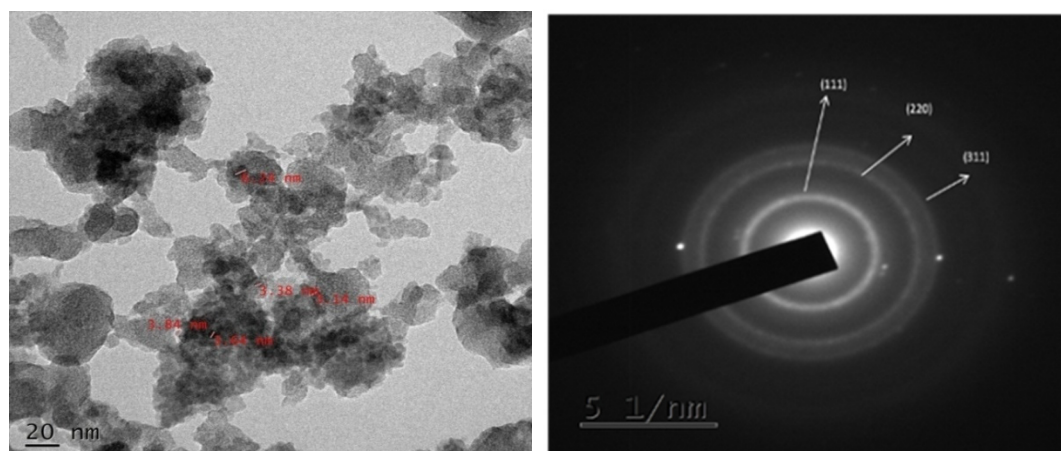Fig. 4. SEM-EDAX images of CdSe (a, b) and Zr-CdSe (c, d) nanoparticles

Fig. 5. TEM image (a) and SAED pattern (b) of Zr doped CdSe nanoparticles

the catalytic surface, it's preventing the reaction between the IC dye molecule and hydroxyl radicals, due to lack of active sites.

2. The concentration of the dye increases in the aqueous solution, it becomes a high-intensity color and not transparent, so the path length of photons entering into the solution decreases [41].

3. Reduced photogeneration of OH and O_2^- radicals on the catalyst surface.

4. Dye molecules are covered on the active site of the

catalyst, which could be reduced the degradation efficiency [42].

Effect of irradiation time

The irradiation time is playing a crucial part in the process of photocatalytic degradation. The result of irradiation time was carried out with a fixed dosage of the catalyst (20mg of CdSe and Zr-CdSe NPs) and the optimum initial concentration of IC dye solution (35ppm). The effect of illuminating
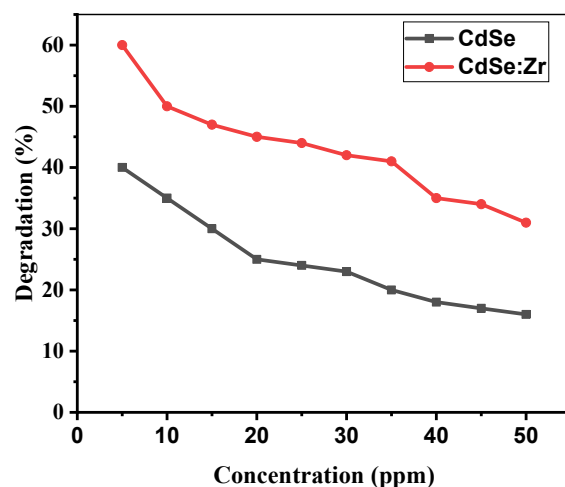
Fig. 6. Effect of initial dye concentration on the photodegradation of IC dye
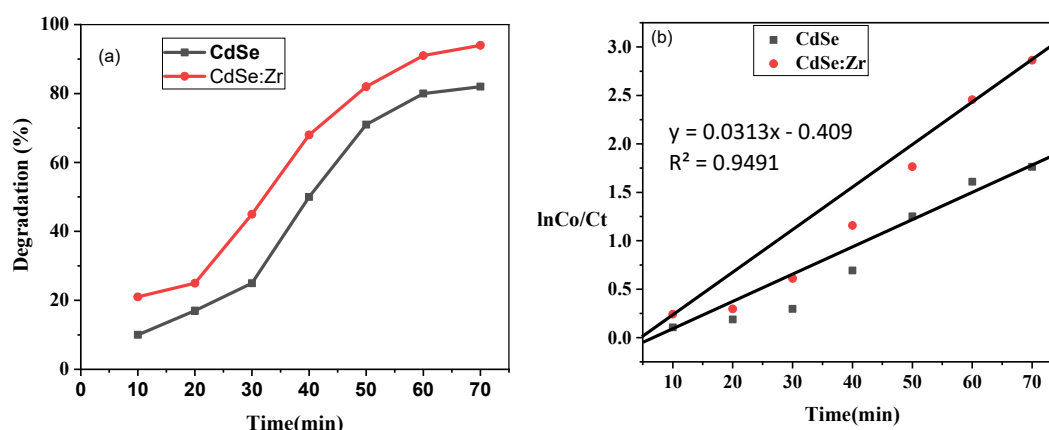

Fig. 7. Effect of irradiation time (a) and photodegradation kinetics (b) of IC dye

time for the degradation of IC dye varies from 10 to 70 min. The percentage of degradation increases from 10% to 82% by increasing irradiation time for CdSe and 21% to 94% for Zr-CdSe nanoparticles which are shown in Fig. 7. This may be due to the sufficient time to have the reacted dye molecules on the catalyst surface and generate hydroxyl, superoxide radicals [41-43]. The concentration of dye solution gradually reduced due to the absorption of dye molecules on empty active sites and finally reached the saturation stage, hence the percentage of degradation increased.

These experimental results show that the photocatalytic degradation of IC dye obeys pseudo-first-order kinetics and the rate is expressed by the following relation

$\ln C_o/C_t = kt$

Where C_o is the initial concentration, C_t is the concentration at time t, k is the pseudo-first-order rate constant and t is the illumination time respectively. The value of $\ln C_o/C_t$ is plotted against the time (in min) and the plot was found to be linear (Fig. 7 (b)). From the slop, the rates constant k was determined for degradation of IC dye in the presence of CdSe and CdSe: Zr. The pseudo-first-order rate constant of CdSe NPs is 0.0313min^{-1} and 0.04325min^{-1} for CdSe: Zr NPs. This indicates the photodegradation efficiency of IC dye is higher in the presence of CdSe: Zr NPs [44].

Effect of amount of photocatalyst

The photocatalytic activity highly depends on the amount of catalyst. The effect of the catalyst amount on the degradation of IC dye was carried out by varying the amount of photocatalyst from 5mg to 40mg/20ml. Fig. 8 showed that the
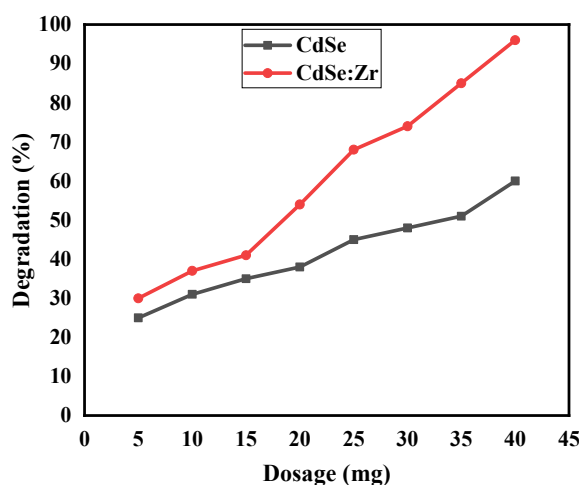
J. Water Environ. Nanotechnol., 6(2): 177-187 Spring 2021

183

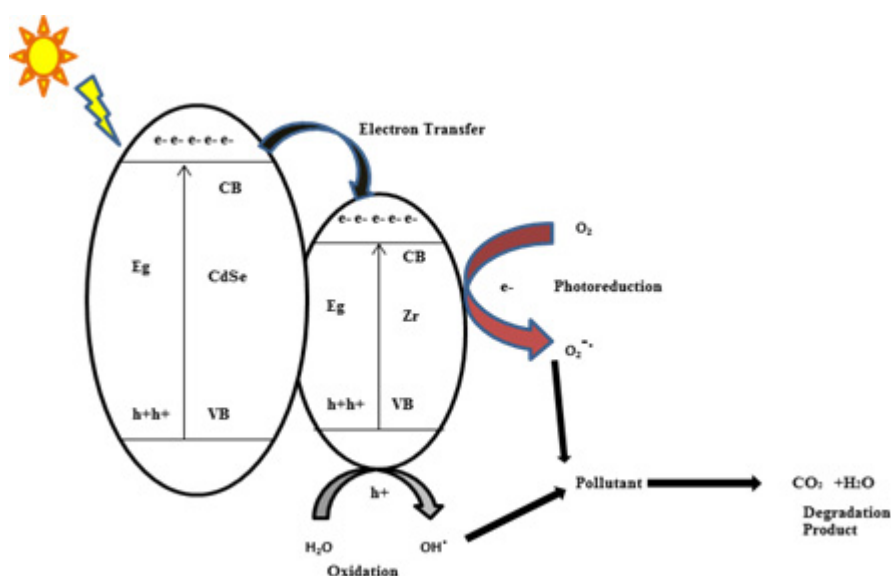Fig. 8. Effect of dose of the catalyst on the photodegradation of IC dye

Fig. 9. Mechanism for the photodegradation of IC dye on Ze-CdSe nanoparticles

percentage of decoloration efficiency increases with the growth in the amount of catalyst from 25% to 60% for CdSe and 30% to 96% for Zr-CdSe NPs under solar illumination. The percentage of decoloration was found to increase linearly with an increase in the amount of the photocatalyst pointing as a heterogeneous regime. This may be due to:

1. The number of surface active sites increases with the increasing amount of photocatalyst leads to the decrease in the penetration effects of radiation due to the shielding effects [41, 42].

2. More number of hydroxyl radicals generated in the aqueous solution due to an increase in the concentration of charge carriers [45].

3. A large number of dye molecules adsorbed on the photocatalytic surface [46].

However, the amount of photocatalyst increase the reaction rate tends to decrease. This may be attributed to 1. Deactivation of activated molecules by collision with ground-state molecules. 2. The excess amount of photocatalytic particles creates the screening effect [47, 48]. 3. The turbidity of the reaction mixture is increasing, which results in the shadowing effect that affects the penetration depth of light illumination [49, 50]. 4. Increasing the effect of scattering and opacity of suspension. Hence the above reason was pointed out the number of

184

J. Water Environ. Nanotechnol., 6(2): 177-187 Spring 2021

catalyst increases; the rate of reaction is reduced.

4.*Photocatalytic degradation mechanism*

The electron transfer mechanism occurs in the presence of Zr doped un-doped CdSe NPs, during photocatalytic degradation of IC Dye under solar light irradiation. When solar light irradiated on the surface of photocatalyst, that promotes the electrons, transfer from valence band to conduction band and it generates an electrons hole-pair. The photo-induced electron can be easily trapped by acceptors such as molecular oxygen forming superoxide radical anion and the holes can easily be trapped by OH⁻ as well as H_2O to produced OH· radicals are shown in Fig. 9. This reaction can be

$$CdSe + hU \longrightarrow h^+(VB) + e^- (CB)$$

$$e^- + O_2 \longrightarrow O_2^{-\cdot}$$

$$h^+ + OH^- \longrightarrow OH^\cdot$$
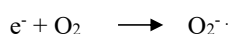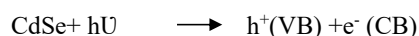
The deposition of transition metals on semiconductor nanoparticles is an effective way for improving photocatalytic efficiency. As transition metals, Zr acts as an electron scavenger and stores them effectively. Since Zr ion has an impact to generate more number of holes and electrons, due to reduced the bandgap. The dopant can reduce the crystallite size and have large surface area properties. Which increases electron transfer properties, enhances the photocatalytic activity.

CONCLUSION

Zirconium doped and un-doped CdSe nanoparticles were successfully synthesized by a simple chemical approach and utilized for photocatalytic degradation of IG dye under solar irradiation. UV- Vis spectra indicated that both zirconium doped and un-doped CdSe nanoparticles have a broad and strong absorption band in the visible range, indicating that the incorporation of Zr ion on the surface of CdSe. The EDAX elemental analysis confirms the presence of Zr ion on the CdSe lattice. The nano-sized particles of zirconium doped and un-doped CdSe nanoparticles were confirmed by SEM and TEM analysis. Photocatalytic activity studies revealed that Zr-doped CdSe possessed greater photocatalytic activity when compared with un-doped CdSe. Kinetics studies indicate the photo decoloration reaction followed pseudo-first-order kinetics.

CONFLICTS OF INTEREST

The authors declare there are no conflicts of interest.

REFERENCES

1. Wang J, He Y, Tao J, He J, Zhang W, Niu S, et al. Enhanced photodegradation of dyes on titania-based photocatalysts by adding commercial GeO2 in aqueous suspension. Chemical Communications. 2010;46(29):5250.

2. Chikate RC, Kadu BS. Improved photocatalytic activity of CdSe-nanocomposites: Effect of Montmorillonite support towards efficient removal of Indigo Carmine. Spectrochimica Acta Part A: Molecular and Biomolecular Spectroscopy. 2014;124:138-47.

3. Hoffmann MR, Martin ST, Choi W, Bahnemann DW. Environmental Applications of Semiconductor Photocatalysis. Chemical Reviews. 1995;95(1):69-96.

4. Lee G-J, Wu JJ. Recent developments in ZnS photocatalysts from synthesis to photocatalytic applications — A review. Powder Technology. 2017;318:8-22.

5. Garcia-Segura S, Brillas E. Applied photoelectrocatalysis on the degradation of organic pollutants in wastewaters. Journal of Photochemistry and Photobiology C: Photochemistry Reviews. 2017;31:1-35.

6. Masih D, Ma Y, Rohani S. Graphitic C3N4 based noble-metal-free photocatalyst systems: A review. Applied Catalysis B: Environmental. 2017;206:556-88.

7. Gaya UI, Abdullah AH. Heterogeneous photocatalytic degradation of organic contaminants over titanium dioxide: A review of fundamentals, progress and problems. Journal of Photochemistry and Photobiology C: Photochemistry Reviews. 2008;9(1):1-12.

8. Yu JC, Yu J, Ho W, Zhang L. Preparation of highly photocatalytic active nano-sized TiO2 particles via ultrasonic irradiation. Chemical Communications. 2001(19):1942-3.

9. Serpone N. Is the Band Gap of Pristine TiO2Narrowed by Anion- and Cation-Doping of Titanium Dioxide in Second-Generation Photocatalysts? The Journal of Physical Chemistry B. 2006;110(48):24287-93.

10. Stylidi M. Pathways of solar light-induced photocatalytic degradation of azo dyes in aqueous TiO2 suspensions. Applied Catalysis B: Environmental. 2003;40(4):271-86.

11. Muhd Julkapli N, Bagheri S, Bee Abd Hamid S. Recent Advances in Heterogeneous Photocatalytic Decolorization of Synthetic Dyes. The Scientific World Journal. 2014;2014:1-25.

12. Othman I, Mohamed RM, Ibrahem FM. Study of photocatalytic oxidation of indigo carmine dye on Mn-supported TiO2. Journal of Photochemistry and Photobiology A: Chemistry. 2007;189(1):80-5.

13. Gemeay AH, Mansour IA, El-Sharkawy RG, Zaki AB. Kinetics and mechanism of the heterogeneous catalyzed oxidative degradation of indigo carmine. Journal of Molecular Catalysis A: Chemical. 2003;193(1-2):109-20.

14. Lo S, Lin C, Wu C, Hsieh P. Capability of coupled CdSe/TiO for photocatalytic degradation of 4-chlorophenol. Journal of Hazardous Materials. 2004;114(1-3):183-90.

15. Yang J, Tang A, Zhou R, Xue J. Effects of nanocrystal size and device aging on performance of hybrid poly(3-hexylthiophene):CdSe nanocrystal solar cells. Solar Energy

J. Water Environ. Nanotechnol., 6(2): 177-187 Spring 2021

185

Materials and Solar Cells. 2011;95(2):476-82.

16. Biswal N, Parida KM. Enhanced hydrogen production over CdSe QD/ZTP composite under visible light irradiation without using co-catalyst. International Journal of Hydrogen Energy. 2013;38(3):1267-77.

17. Huynh WU, Peng X, Alivisatos AP. CdSe Nanocrystal Rods/Poly(3-hexylthiophene) Composite Photovoltaic Devices. Advanced Materials. 1999;11(11):923-7.

18. Robel I, Subramanian V, Kuno M, Kamat PV. Quantum Dot Solar Cells. Harvesting Light Energy with CdSe Nanocrystals Molecularly Linked to Mesoscopic TiO2Films. Journal of the American Chemical Society. 2006;128(7):2385-93.

19. Zhou M, Han D, Liu X, Ma C, Wang H, Tang Y, et al. Enhanced visible light photocatalytic activity of alkaline earth metal ions-doped CdSe/rGO photocatalysts synthesized by hydrothermal method. Applied Catalysis B: Environmental. 2015;172-173:174-84.

20. Fujishima A, Zhang X, Tryk D. Heterogeneous photocatalysis: From water photolysis to applications in environmental cleanup. International Journal of Hydrogen Energy. 2007;32(14):2664-72.

21. Miyazaki H, Matsui H, Kuwamoto T, Ito S, Karuppuchamy S, Yoshihara M. Synthesis and photocatalytic activities of MnO2-loaded Nb2O5/carbon clusters composite material. Microporous and Mesoporous Materials. 2009;118(1-3):518-22.

22. Miyazaki H, Matsui H, Karuppuchamy S, Uchizumi J, Ito S, Yoshihara M. Synthesis and characterization of Ta2O5/HfO2/carbon clusters composite materials. Materials Chemistry and Physics. 2009;113(1):36-41.

23. Charanpahari A, Umare SS, Gokhale SP, Sudarsan V, Sreedhar B, Sasikala R. Enhanced photocatalytic activity of multi-doped TiO2 for the degradation of methyl orange. Applied Catalysis A: General. 2012;443-444:96-102.

24. Anni Kausalya, J., V. Joseph and S. Krishnakumar,2013. Synthesis of Cadmium Selenide Nanoparticles by Wet Chemical Method. Elixir Applied Chemistry, 55(A): 13036-13038.

25. Shams-Nateri A., 2011. Dye Concentration Determination in Ternary Mixture Solution by using Colorimetric Algorithm, Iran Journal of Chemistry. Chemical Engineering, 30(4): 51-61.

26. Kristl M, Ban I, Danč A, Danč V, Drofenik M. A sonochemical method for the preparation of cadmium sulfide and cadmium selenide nanoparticles in aqueous solutions. Ultrasonics Sonochemistry. 2010;17(5):916-22.

27. Chen M-L, Oh W-C. Synthesis and highly visible-induced photocatalytic activity of CNT-CdSe composite for methylene blue solution. Nanoscale Research Letters. 2011;6(1).

28. Zhao W-B, Zhu J-J, Chen H-Y. Photochemical preparation of rectangular PbSe and CdSe nanoparticles. Journal of Crystal Growth. 2003;252(4):587-92.

29. A Book: Willson, A.J.P., 1963. Mathematical Theory of X-ray Powder Diffractometry. Gordon & Breach. New York.

30. Leena AMB, Raji K. Photocatalytic Activity of Pure and Nickel Doped Cadmium Sulphide Nanoparticles Synthesized via Co-Precipitation Method. Volume 5, Issue 2. 2019;5(3):710-2.

31. Lin J, Yu JC. An investigation on photocatalytic activities of mixed TiO2-rare earth oxides for the oxidation of acetone in air. Journal of Photochemistry and Photobiology A: Chemistry. 1998;116(1):63-7.

32. Nehru, L .C., V. Swaminathan , C. Sanjeeviraja, 2006. Photoluminescence Studies on Nanocrystalline Tin Oxide Powder for Optoelectronic Device. Journal of Material Science, 2(2): 6-10.

33. Velumani, S., X. Mathew, P.J. Sebastian, S.K. Narayandass and D. Mangalaraj, 2003. Structural and Optical Properties of Hot Wall Deposited CdSe Thin Films. Solar Energy Materials and Solar Cell, 76(3): 347-358.

34. A Book: Culity, B.D and S.R. Stock, 2001. Elements of X-ray Diffraction 3rd edition. Prentice Hall. Upper Saddle river (Do1)

35. Singh S, Rath MC, Singh AK, Mukherjee T, Jayakumar OD, Tyagi AK, et al. CdSe nanoparticles grown via radiolytic methods in aqueous solutions. Radiation Physics and Chemistry. 2011;80(6):736-41.

36. A Book: Woggon.U, 1997. Springer Tracts in Modern Physics, 136.

37. A Book: Tauc, J., 1974. Amorphous and liquids semiconductors. Plenium press. New York.

38. Mahmoud WE, Al-Amri AM, Yaghmour SJ. Low temperature synthesis of CdSe capped 2-mercaptoethanol quantum dots. Optical Materials. 2012;34(7):1082-6.

39. Yadav K, Dwivedi Y, Jaggi N. Structural and optical properties of Ni doped ZnSe nanoparticles. Journal of Luminescence. 2015;158:181-7.

40. Limaye MV, Singh SB, Date SK, Gholap RS, Kulkarni SK. Epitaxially grown zinc-blende structured Mn doped ZnO nanoshell on ZnS nanoparticles. Materials Research Bulletin. 2009;44(2):339-44.

41. Muthirulan P, Meenakshisundararam M, Kannan N. Beneficial role of ZnO photocatalyst supported with porous activated carbon for the mineralization of alizarin cyanin green dye in aqueous solution. Journal of Advanced Research. 2013;4(6):479-84.

42. Muthirulan, P., G. Naganthan, M. Meenakshi Sundaram and N. Kannan, 2012. Beneficial Role of Commercial Activated Carbon for the Decoloration of Safranine Dye on TiO2 and ZnO/UV System for the Application of Effluents Treatment from Waste Water. Indian Journal of Environmental Protection, 32: 546-553.

43. Devi LG, Kumar SG. Influence of physicochemical–electronic properties of transition metal ion doped polycrystalline titania on the photocatalytic degradation of Indigo Carmine and 4-nitrophenol under UV/solar light. Applied Surface Science. 2011;257(7):2779-90.

44. Wang F, Zhang K. Reduced graphene oxide–TiO2 nanocomposite with high photocatalystic activity for the degradation of rhodamine B. Journal of Molecular Catalysis A: Chemical. 2011;345(1-2):101-7.

45. Lakshmi UR, Srivastava VC, Mall ID, Lataye DH. Rice husk ash as an effective adsorbent: Evaluation of adsorptive characteristics for Indigo Carmine dye. Journal of Environmental Management. 2009;90(2):710-20.

46. Wang W-S, Wang D-H, Qu W-G, Lu L-Q, Xu A-W. Large Ultrathin Anatase TiO2 Nanosheets with Exposed {001} Facets on Graphene for Enhanced Visible Light Photocatalytic Activity. The Journal of Physical Chemistry C. 2012;116(37):19893-901.

47. Chen C, Liu J, Liu P, Yu B. Investigation of Photocatalytic Degradation of Methyl Orange by Using Nano-Sized ZnO Catalysts. Advances in Chemical Engineering and Science. 2011;01(01):9-14.

186

J. Water Environ. Nanotechnol., 6(2): 177-187 Spring 2021

48. Daneshvar N, Salari D, Khataee AR. Photocatalytic degradation of azo dye acid red 14 in water on ZnO as an alternative catalyst to TiO2. Journal of Photochemistry and Photobiology A: Chemistry. 2004;162(2-3):317-22.

49. Pastrana-Martínez LM, Morales-Torres S, Likodimos V, Figueiredo JL, Faria JL, Falaras P, et al. Advanced nanostructured photocatalysts based on reduced graphene oxide–TiO2 composites for degradation of diphenhydramine pharmaceutical and methyl orange dye. Applied Catalysis B: Environmental. 2012;123-124:241-56.

50. Yoo D-H, Cuong TV, Pham VH, Chung JS, Khoa NT, Kim EJ, et al. Enhanced photocatalytic activity of graphene oxide decorated on TiO2 films under UV and visible irradiation. Current Applied Physics. 2011;11(3):805-8.

J. Water Environ. Nanotechnol., 6(2): 177-187 Spring 2021

187